sustainability

MDPI

Article

High-Resolution UAV-Based NDVI Monitoring Method for Sustainable Post-Mining Land Management

Bartosz Orzeł [1], Michail Galetakis [2,*], Dariusz Michalak [1], Jarosław Tokarczyk [1], Kamil Szewerda [1], Magdalena Rozmus [1], Emmanouil A. Varouchakis [2] and Georgios Xiroudakis [2]

[1] KOMAG Institute of Mining Technology, Pszczyńska 37, 44-101 Gliwice, Poland; borzel@komag.eu (B.O.); dmichalak@komag.eu (D.M.); jtokarczyk@komag.eu (J.T.); kszewerda@komag.eu (K.S.); mrozmus@komag.eu (M.R.)

[2] School of Mineral Resources Engineering, Technical University of Crete, 73-100 Chania, Greece; evarouchakis@tuc.gr (E.A.V.); gxiroudakis@tuc.gr (G.X.)

* Correspondence: mgaletakis@tuc.gr

Abstract

The transition of coal regions under the European Green Deal and Just Transition Fund creates a need for quantitative, transparent monitoring of ecological recovery on post-mining land. This study presents an autonomous UAV-based methodology for high-resolution monitoring of vegetation dynamics on a reclaimed coal waste heap in Upper Silesia, Poland. A DJI Mavic 3 Multispectral platform with RTK positioning conducted approximately biweekly flights from August 2024 to October 2025 over three study plots acquiring RGB and multispectral imagery at approximately 4 cm/pixel. Photogrammetric processing in DJI Terra produced radiometrically corrected orthomosaics and NDVI maps, which were analyzed using an automated QGIS workflow for reprojection, clipping, NDVI-based classification, and quantification of vegetation area across three different reclamation variants. The results indicate that intensive soil conditioning through the application of compost derived from bio-waste achieved a maximum vegetation cover of 94.4%. This treatment consistently maintained the highest level of cover during periods of environmental stress and significantly surpassed both seeding-only treatments and those combining seeding with irrigation. Baseline vegetation cover below 6% confirmed the necessity of active reclamation. This workflow provides rapid and reproducible metrics that are suitable for adaptive management and regulatory reporting. It also offers a scalable template for monitoring coal waste heaps across Europe undergoing SDG-aligned reclamation.

Keywords: post-mining; land reclamation; vegetation monitoring; drone; multispectral imaging; NDVI; sustainability; sustainable ecosystems; sustainable land management

Check for updates

Academic Editor: Teodor Rusu

Received: 27 February 2026
Revised: 26 April 2026
Accepted: 30 April 2026
Published: 6 May 2026

1. Introduction

The transformation of coal-dependent regions in the European Union is guided by the European Green Deal and the Just Transition Mechanism [1,2]. These areas face significant environmental challenges, including soil contamination, altered hydrology, landscape instability, and biodiversity loss [3,4]. Reclamation aims to restore such environments into stable and self-sustaining ecosystems, where vegetation establishment plays a key role in soil stabilization, water regulation, and ecological recovery [5–11].

Transforming post-mining areas into sustainable ecosystems through ecological restoration is consistent with Sustainable Development Goals (SDGs) [12]. Establishment of sustainable vegetation on post-mining lands:

- Meets SDG 15 (Life on Land), particularly Targets 15.1 (ecosystem conservation/restoration) and 15.3 (degraded land and soil restoration);
- Enhances carbon sequestration and reduces soil erosion, supporting SDG 13 (Climate Action) [1], Target 13.1 (strengthen resilience to climate hazards);
- Supports SDG 11 (Sustainable Cities and Communities), and Target 11.7 (green and public spaces) in particular.

This requires effective, quantitative, and reproducible monitoring methods.

Monitoring vegetation dynamics is essential for assessing the effectiveness of reclamation strategies, including soil amendments, plant species selection, and fertilization regimes. Although ground-based methods can provide accurate measurements, they are typically labor-intensive and limited in spatial and temporal coverage [13,14]. Modern approaches increasingly use remote sensing, including satellite imagery and the application of unmanned aerial vehicles, as well as GIS-based analyses, for this purpose. However, these tools are not yet routinely implemented across reclamation projects.

Remote sensing-based vegetation assessment relies on well-established principles of plant spectral response to electromagnetic radiation [15,16]. The contrast between red and near-infrared reflectance enables the calculation of vegetation indices such as the Normalized Difference Vegetation Index (NDVI), which is widely used for quantifying vegetation conditions and dynamics [17–20]. Satellite imagery has been extensively applied in post-mining environments [21–33]. However, its effectiveness is constrained by spatial resolution limitations, revisit frequency, and cloud cover. These factors reduce its suitability for monitoring small and heterogeneous sites [34,35].

An alternative remote sensing solution for collecting data to monitor the revegetation progress is the use of unmanned aerial vehicles (UAV, hereafter referred to as "drone") [35–47]. UAV technology has evolved from simple aerial photography platforms to sophisticated remote sensing systems capable of collecting scientifically robust multispectral data across diverse environmental conditions. Moreover, recent advances in positioning technologies, including Real-Time Kinematic (RTK) and Networked Transport of RTCM via Internet Protocol (NTRIP), have enabled centimeter-level georeferencing accuracy without the need for ground control points [48–53]. Furthermore, contemporary photogrammetric software and GIS platforms facilitate automated and reproducible processing of multispectral data, thereby enabling quantitative analysis of vegetation dynamics.

These technological developments enable more efficient and adaptive management of reclamation processes by allowing rapid assessment of vegetation establishment, identification of areas requiring intervention, and evaluation of treatment effectiveness. Furthermore, high-resolution UAV data contributes to improved understanding of ecosystem recovery processes in post-mining environments.

In this context, the present study proposes a UAV-based methodology for high-resolution monitoring of vegetation dynamics on reclaimed mine heaps. The approach integrates multispectral data acquisition at approximately 4 cm/pixel resolution with an automated QGIS-based workflow for NDVI analysis and vegetation area quantification. The study was conducted on a reclaimed mine heap in Rybnik, Poland, where a range of reclamation treatments were evaluated. The objectives of this study are to develop an automated UAV–QGIS workflow for NDVI-based vegetation assessment at plot scale and to assess vegetation cover dynamics across different reclamation treatments during the monitoring period.

Based on the above, this paper is structured as follows. Section 2 provides an overview of recent developments in UAV-based monitoring of post-mining environments, with particular emphasis on multispectral remote sensing and NDVI-based vegetation assessment. Section 3 describes the study area, experimental design, UAV data acquisition and the automated UAV–QGIS workflow developed for processing multispectral imagery and quantifying vegetation cover at plot scale. Section 4 presents the results of the multi-temporal monitoring campaign, highlighting differences in vegetation dynamics among reclamation treatments. Finally, Section 5 summarizes the main conclusions and suggests future research directions.

2. UAV-Based Monitoring in Post-Mining Areas

Modern multispectral systems deployed on UAVs typically integrate Red–Green–Blue (RGB) cameras alongside dedicated multispectral sensors that capture data in narrow spectral bands encompassing the red (620–750 nm), red-edge (700–750 nm), and near-infrared (NIR; 750–1400 nm) regions. Emerging hyperspectral systems, increasingly employed in international applications, capture over 150 narrow spectral bands, enabling detection of advanced vegetation properties such as hydration stress, nutrient concentration, and contaminant presence. These advanced spectral capabilities form the foundation for calculating vegetation indices, with the Normalized Difference Vegetation Index (NDVI) remaining the most widely applied metric in global post-mining reclamation monitoring applications. In heterogeneous post-mining environments, where variable soil colors, coal residues, and exposed mineral surfaces produce diverse spectral reflectance properties, hyperspectral systems enable more precise characterization of post-industrial substrates and can reveal vegetation stress caused by heavy metal contamination or acid mine drainage.

For successful reclamation, a comprehensive view of the subjected land must be identified. Advanced systems deployed in international reclamation projects also include thermal cameras, which can support monitoring of temperature conditions in volcanic or thermal areas and identify self-heating coal ash areas representing significant hazards in coal heaps [54–56].

Recent developments in post-mining and post-industrial monitoring include integration of machine learning models to automate image analysis and support decision-making [57–59]. In South Africa, research utilizing Faster R-CNN and Mask R-CNN (recurrent convolutional neural network) models to identify mining waste storage facilities (tailings storage facilities, TSF) on Sentinel-2 satellite images demonstrated the capability to detect 46 TSF facilities not included in training data, with accuracy exceeding 67%. These deep neural network models can extract higher-dimensional and more abstract image features than traditional methods, proving to be a powerful technology for processing remote sensing imagery [60]. In China, machine learning models such as Gradient Boosting Decision Tree (GBDT) demonstrated superior predictive accuracy in estimating soil cadmium concentrations by integrating multi-source UAV data (multispectral images, digital terrain models, and RGB orthophotos) with machine learning algorithms [61]. A case study from Garzweiler II in Germany illustrates the practical application of UAVs for monitoring terrain displacements induced by mining near the Viersen zone of the mining operation [62]. Multi-sensor UAV monitoring included simultaneous collection of multispectral RGB, thermal, and spectral data, enabling identification of both topographic surface deformations and potentially active fault structures with spatial resolution sufficient to identify surface cracks.

3. Materials and Methods

A comprehensive survey of active and reclaimed post-mining waste dumps owned by the Polish mining and energy company PGG (Polska Grupa Górnicza S.A., Katowice, Polska) was conducted. Initially, five promising sites among PGG landfills were chosen as shown in Figure 1:

- KWK Sośnica (point 1);
- KWK ROW Ruch Chwałowice (point 2);

- KWK ROW Ruch Rydułtowy (point 3);
- KWK ROW Ruch Marcel (point 4);
- KWK ROW Ruch Jankowice (point 5).

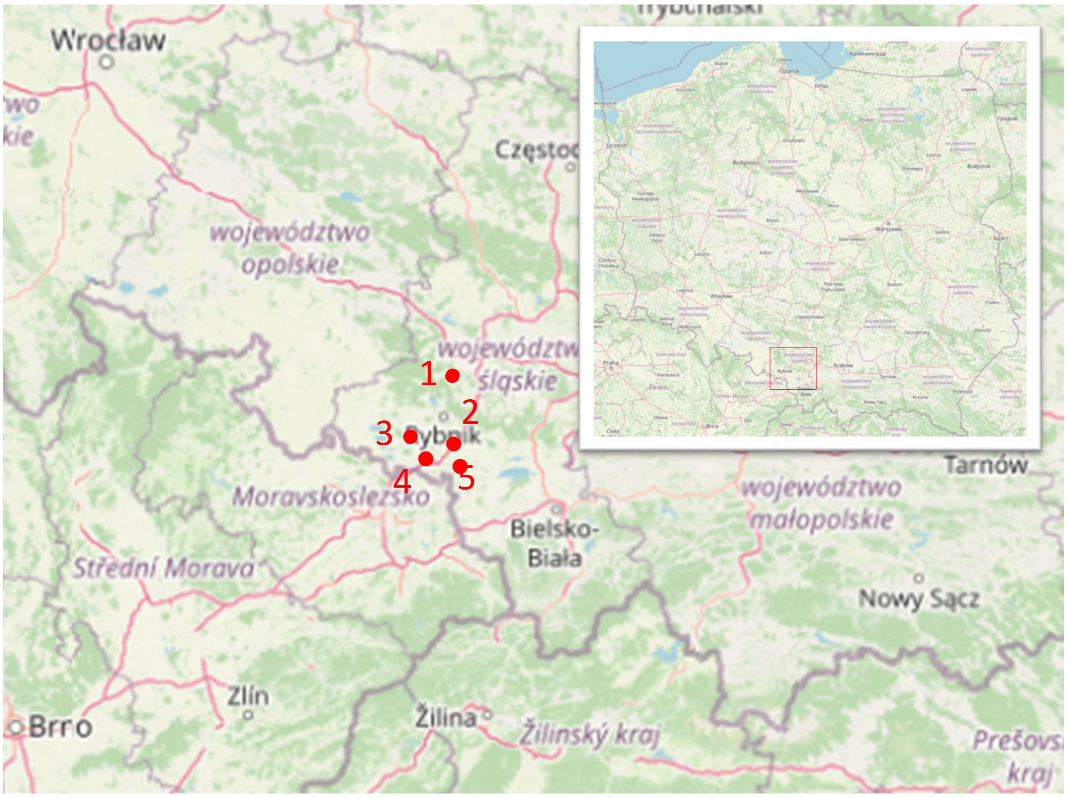

Figure 1. Locations of the initially selected post-mining waste landfills in Poland belonging to PGG S.A. (1 = KWK Sośnica, 2 = KWK ROW Ruch Chwałowice, 3 = KWK ROW Ruch Rydułtowy, 4 = KWK ROW Ruch Marcel and 5 = KWK ROW Ruch Jankowice). The area including the post-mining waste landfills is shown in the overlapping map of Poland by the red rectangle.

Prior to establishing the study fields, a thorough on-the-ground and remote assessment of the candidate locations was conducted. The shape and gradient of the terrain, ease of access for equipment and personnel, and the observed state of plant succession were considered. Ultimately, the northern sector of the KWK ROW Ruch Jankowice landfill was selected, due to its stabilized structure and the emergence of native vegetation, providing a representative setting for advanced reclamation trials.

The chosen area for the Jankowice mine heap study area in the shape of a rectangle 40 m × 60 m is presented in Figure 2 (green rectangle).

Prior to the commencement of the observations, a reference flight was conducted on 1 August 2024, to collect baseline data in the form of orthophotos and multispectral maps (RGB, NDVI). This data was then used as a reference point to assess the dynamics of changes in the subsequent weeks of monitoring. The primary rationale behind the selection of this mine heap is as follows:

- Substrate stability: It is a relatively flat area with stabilized flotation tailings.
- Initial vegetation cover: The presence of spontaneous pioneer vegetation serves as a reference point for experiments.
- Representativeness: The typical characteristics of mine heaps in Upper Silesia.
- Accessibility: The possibility of conducting long-term research with access to mining infrastructure.

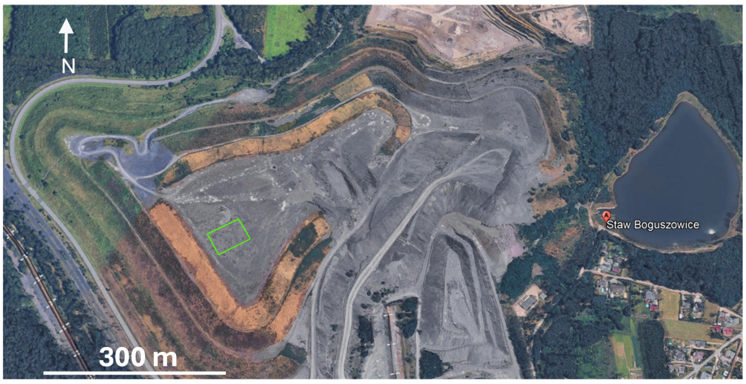

Figure 2. View of the greater area of Jankowice spoil heap. The area including the study plots is shown by the green rectangle.

The stability of the substrate was examined based on terrain slopes and site familiarity. This was ensured through analysis of data provided by the mineral processing plant to which the heap belongs.

Landscape documentation in the form of othophotomaps stitched from high-resolution aerial imagery was developed using a DJI Mavic 3 Multispectral drone platform and DJI Terra V5.2.0. software (See Supplementary Materials).

The initial level of greenness (vegetation) and the determination of the need for further research and reclamation works were assessed using the NDVI:

$$NDVI = \frac{NIR - RED}{NIR + RED} \quad (1)$$

where

NIR: Value of reflectance in the near-infrared range;
RED: Value of reflectance in the red part of the spectrum.

The NDVI calculation allows a quantitative assessment of photosynthesis intensity and distinguishes surfaces covered with actively green vegetation.

In the designated study area, three study plots (A, B and C) were identified, exhibiting a semi-circular configuration (see Figure 3). This was undertaken in consideration of the implementation of rotating spraying apparatus for the purpose of revegetation. This automated spraying system has been developed for the purpose of applying remediation mixtures, including water, seeded mulch and organic biofertilisers, in degraded post-mining areas. The key operating element is a rotating spray cannon equipped with two independent nozzles, enabling the application of media with varying densities and the adjustment of spray characteristics [63]. Therefore, the precise delineation of both the outer and inner boundaries of these plots was necessary.

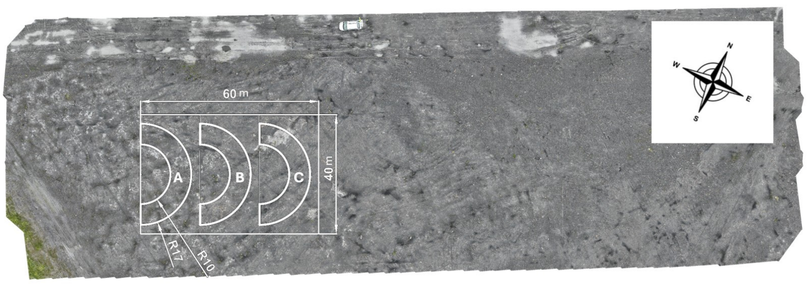

Figure 3. The location of the 3 study plots within the mine heap. The details of the semi-circular configuration of study plots (A, B and C) are shown.

The study plots were subjected to different methods of recultivation treatments as shown in Table 1.

Table 1. Study plots and methods of recultivation treatments.

Plot ID	Plot Area (m^2)	Reclamation Treatment	Soil Amendment	Irrigation	Key Objective
A	297	Seeding only	None	No	Baseline revegetation without intervention
B	297	Seeding and irrigation	None	Yes	Assess effect of water supplementation
C	297	Seeding and compost amendment	Compost from bio-waste	No	Evaluate impact of soil conditioning

For Plot C, soil conditioning used a specially developed compost comprising brown coal and organic waste (chicken feathers and straw), enhanced by active microorganisms via biosolubilization.

The research plan comprised approximately biweekly assessments of plant growth dynamics across the study area. The first calibration flight utilizing a multispectral drone (a DJI drone equipped with a multispectral camera) was conducted on 1 August 2024, even prior to the introduction of seeds, thus providing a robust baseline for subsequent spectral analyses. The planned monitoring sequence started on 8 May 2025 and continued through 31 July 2025, with drone flights conducted approximately every fourteen days to ensure high temporal resolution in data acquisition. Details and photos of used equipment are included in the Supplementary Materials.

The implementation of regular drone flights facilitates cyclical monitoring of the vegetation condition at the designated study plots and was used to study the suitability of the chosen seed mixture and treatments for the revegetation. Using the UAV-mission planner built into the drone controller, each flight mission was planned adjusting parameters so that they would align seamlessly with the geometric blueprint of the study area. Altitude, trajectory overlap and specific waypoints were all fine-tuned in advance to ensure the drone's path would provide even coverage and minimize errors during multispectral data collection flights. In each mission, the UAV software's automation features were utilized, resulting in the drone accurately executing its designated flight and systematically collecting data for subsequent spectral analysis. The flight lines were planned to adjust to the geometry of the mapped field. The following parameters were used:

- Flight altitude: 20 m;
- Image overlap: 80% forward, 70% side;
- UAV speed: 3.5 m/s;
- Sensor calibration and radiometric correction using UAV software (DJI Terra).

Images were captured at a resolution of 4 cm per pixel, a level of detail selected to unveil even small differences in plant growth.

The UAV flight plan was designed to maximize measurement accuracy and operational efficiency by using flight paths oriented linearly to each other and perpendicular to the boundaries of the study area. To minimize image distortion and varying illumination near the study plots' boundaries, a buffer zone was defined around the study area. The buffer ensures that only the inner part of the area is used for quantitative analyses, eliminating boundary artifacts. The path-planning interface is shown in the Supplementary Materials.

Since the flying path was designed for observation purposes, the following criteria were considered [64–67]:

- Optimization of UAV coverage: The shapes ensure uniform area coverage with constant flight parameters.
- Standardization of procedures: Compliance with agricultural and forestry monitoring protocols.
- Logistical efficiency: Minimization of flight time while maximizing the area covered by the study.
- Georeferencing accuracy: This facilitates precise GPS positioning for measurement repeatability.

The use of straight-line trajectories (Figure 4) also contributes to efficient drone operation by reducing unnecessary maneuvers, thereby saving battery life and shortening mission time. The application of fixed, repeatable flight patterns ensures that each survey is conducted under nearly identical conditions. This consistency facilitates precise temporal comparisons and high reproducibility of results, which are vital for the effective monitoring of vegetation changes on reclaimed post-mining sites.

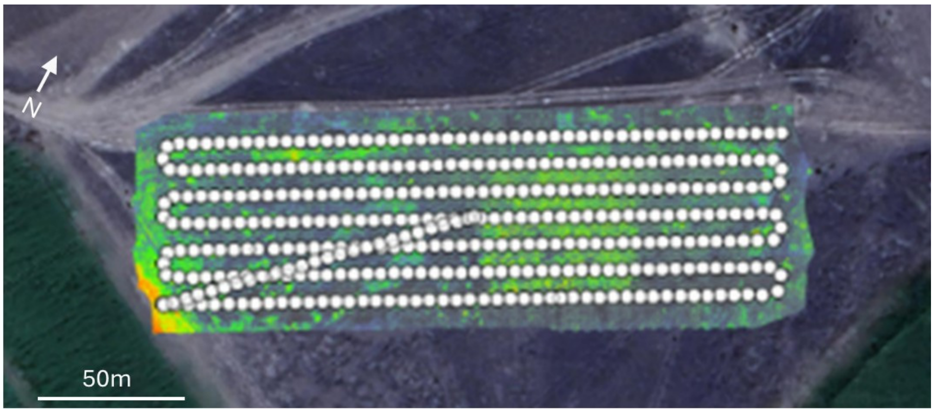

Figure 4. Flight path over the chosen mine heap and resulting multispectral orthophoto image.

The subsequent stage of the process involved the processing of photographs using the drone software (DJI Terra). Establishing an appropriate coordinate system is essential for subsequent NDVI calculations. In this study, the EPSG:2177 coordinate system was utilized. The NDVI processing workflow was implemented in the open-source QGIS (version 3.40) environment using the QGIS Modeler to ensure automated, reproducible, and spatially consistent analysis of high-resolution drone-derived orthophotomaps. The methodology follows a structured sequence of geoprocessing steps, organized into distinct processing phases from data input to quantitative output.

As shown in Figure 5, the workflow begins with the import of four primary input datasets, including: (i) the polygon layer defining the study plots, (ii) the predefined NDVI coloring style, (iii) the NDVI raster map, and (iv) the corresponding RGB raster map. Prior to importing, NDVI rasters are exported as GeoTIFF to preserve spatial reference information and metadata integrity.

To ensure spatial consistency, both NDVI and RGB rasters undergo reprojection to match the coordinate reference system (CRS) of the study plot layer. The reprojected rasters are subsequently clipped to the study plot boundaries, eliminating extraneous data and restricting further computation to the area of interest. The NDVI raster is then symbolized using the predefined NDVI coloring style, and the processed layer is loaded for analysis.

Vegetation identification is performed using the Raster Calculator tool. Pixels corresponding to vegetated surfaces are extracted by applying a predefined NDVI threshold (e.g., NDVI $\geq$ 0.2). The output is a binary raster in which vegetated pixels are assigned a value of "1" and non-vegetated pixels a value of "0". A raster unique values report is subsequently generated to quantify the number of pixels in each class. Based on pixel resolution and spatial extent, the total area covered by vegetation is calculated and exported in JSON format for further statistical processing and reporting.

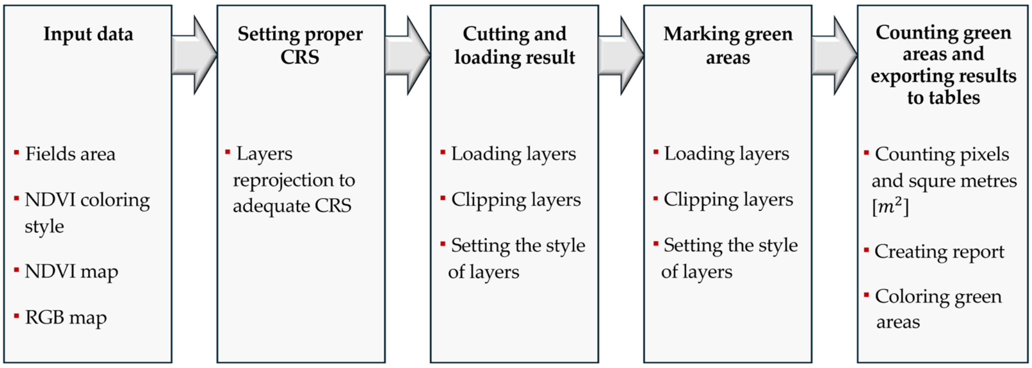

Figure 5. Diagram showing the steps for NDVI calculation using QGIS.

In addition to binary classification, the workflow performs a multi-class aggregation of NDVI values into predefined intervals (e.g., 0.1 to 0.3). A second unique values report summarizes pixel counts and corresponding surface areas for each NDVI class, enabling a more detailed assessment of vegetation vigor and spatial variability within the study plots.

Throughout execution, GDAL (Geospatial Data Abstraction Library) processing logs document input and output file paths, CRS definitions, pixel resolution, and clipping extents, ensuring transparency and reproducibility. The model interface separates input parameters from execution logs, facilitating verification and troubleshooting of intermediate steps. The final outputs consist of two attribute tables summarizing raster-based classification results, one binary and one multi-class, providing a robust quantitative basis for vegetation monitoring and comparative spatial analysis (see the resulting screenshots in the Supplementary Materials).

4. Results—Discussion

The designed automated UAV–QGIS workflow captured distinct temporal patterns of vegetation over 16 months of observations in the study plots. Based on data processing in QGIS software, the vegetation cover, expressed as percentage of area with NDVI ≥ 0.2, has been calculated for each of the study plots. In Figure 6 a typical image of an NDVI map for the three study plots (A, B and C) is shown.

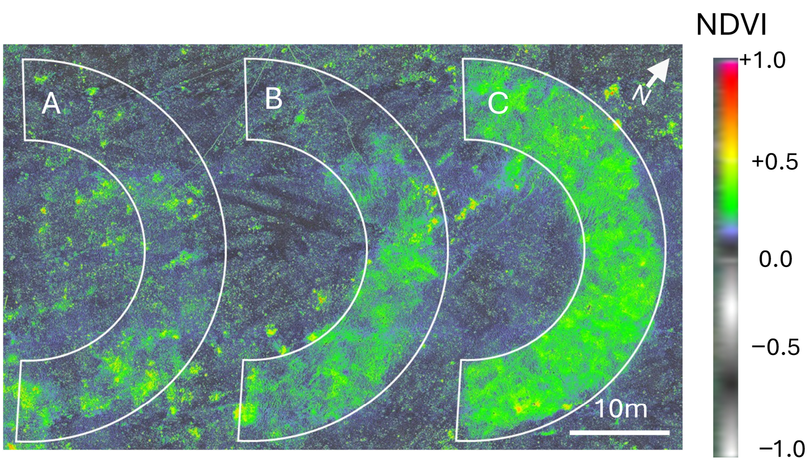

Figure 6. Typical NDVI map for the three study plots (A, B and C). The NDVI of Plot C (compost-amended treatment) is higher than Plot B (seeding with irrigation treatment) and Plot A (seeding-only treatment).

The boxplot of Figure 7 illustrates the distribution of vegetation cover percentage across the full monitoring period for Plots A, B, and C. It summarizes median values, interquartile ranges, and extreme observations (minimum and maximum), thus reflecting both treatment effectiveness and temporal variability.

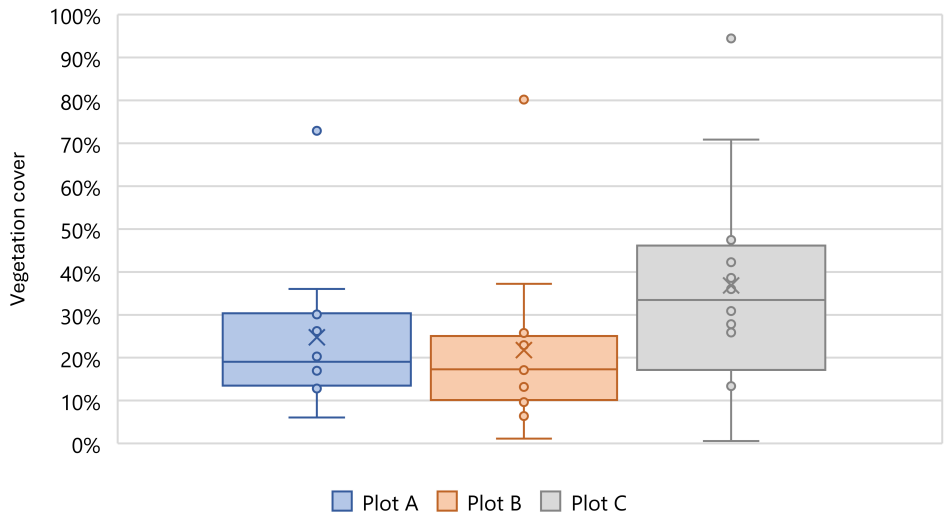

Figure 7. Boxplot showing the variation in the percentage of area with NDVI ≥ 0.2 for the 3 studied plots. Vegetation cover of Plot C (compost-amended treatment) is higher compared to Plot B (seeding with irrigation treatment) and to Plot A (seeding-only treatment).

The boxplot analysis of vegetation cover reveals clear treatment-dependent differences in revegetation performance across the three study plots. Compost-amended Plot C surpassed the other treatments in both the extent and physical intensity of vegetation. It exhibited the highest median vegetation cover, reaching 94.4% (peak) in late July, indicating rapid and extensive covering development.

In contrast, Plot B (seeding with watering) showed moderate improvement relative to Plot A (seeding only), achieving a maximum cover of 80.2%, while Plot A remained the least effective treatment overall. The distribution patterns highlight not only differences in peak performance but also in stability and resilience. Plot A displayed lower median values and a relatively compressed interquartile range at the lower end of the distribution, indicating prolonged periods of limited vegetation establishment. Plot B demonstrated a median similar to Plot A, but with a higher maximum value and symmetrical interquartile range. However, neither Plot A nor Plot B approached the overall performance level of Plot C, which indicated the higher median.

These findings were also statistically validated by conducting the Mood median test and examining the hypothesis that the medians of the three studied plots were equal. Mood's median test is a robust non-parametric statistical method used to compare the medians of two or more independent samples. It evaluates whether samples originate from populations with equal medians by comparing group data against a single, overall median using a chi-square test, making it ideal for skewed data or data with outliers [68]. The resulting p-value (0.097) indicated that the median of Plots A and B are significantly different from the median of Plot C at the 90.0% confidence level.

Consequently, the compost-amended treatment resulted in greater areal coverage, suggesting that substrate conditioning through organic amendment substantially enhances nutrient availability and moisture retention, which are critical factors in post-mining environments characterized by poor soil structure and low fertility.

Regarding the temporal variability, as shown in Figure 8, all treatments exhibited synchronized seasonal dynamics within a single growing period, with rapid expansion from May to July and a pronounced decline during August. More specifically during the period from August 2024 to May 2025, all three plots exhibited relatively modest vegetation coverage. Between May and July 2025, all three plots simultaneously enter a phase of rapid vegetation expansion. This synchronized surge is particularly evident in the steep gradient of all three curves between June and July 2025. Plot C exhibits the most intense proportional increase, rising from approximately 1 m^2 in May to 265 m^2 by July, representing an approximately 200-fold expansion in NDVI-derived coverage area. Plot B demonstrates comparable intensity, achieving 225 m^2 by July, while Plot A reaches 54 m^2 during the same period. The temporal coincidence of this acceleration across all plots suggests a unified response to favorable environmental conditions—likely the conjunction of optimal photoperiod, temperature regime, and soil moisture availability characteristics of mid-summer in the temperate zone.

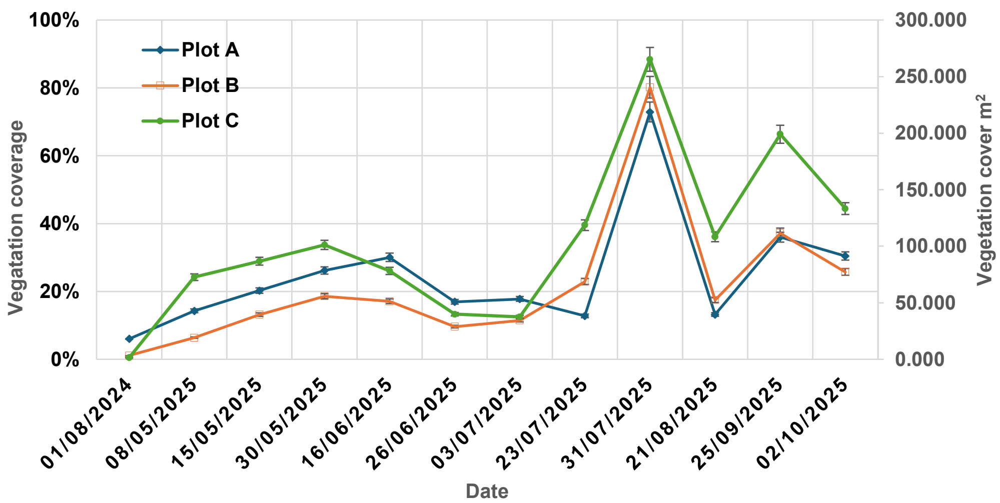

Figure 8. Temporal variation in the percentage of area with NDVI $\geq$ 0.2 for the 3 studied plots (A, B, C) showing the seasonal vegetation development dynamics within a growing period. Compost-amended treatment (Plot C) maintained the highest level of cover during monitoring period and significantly surpassed both seeding-only treatments (Plot A) and treatment combining seeding with irrigation (Plot B). The error bars represent the estimation of vegetation cover at 95% confidence interval.

Following the July 2025 maximum, all three plots exhibit a sharp decline in NDVI-derived coverage area during August 2025, with Plot C experiencing the most intense reduction. This steep post-peak decline is consistent with natural phenological transitions in temperate vegetation, reflecting the transition from active growth to senescence and dormancy as day length decreases and temperatures decline. However, in this case, the occurrence of high temperatures and draughts contributed to the situation. In particular, the total rainfall in the area encompassing the study plots was 123 mm in July 2026, whereas in August of the same year, it was limited to 25.3 mm. By September 2025, Plots A and B had stabilized at approximately 10–20 m^2, suggesting entry into a stable maintenance phase. The differential rate of decline observed among the plots, with Plot C demonstrating a more pronounced reduction in comparison to Plots A and B, may suggest differential frost sensitivity or alternative physiological responses to the onset of autumn conditions.

Table 2 contains vegetation coverage measurements from plots conducted across four key phenological phases between August 2024 and August 2025. Measurements reflect the dynamic plant succession typical of ecosystem regeneration processes in reclaimed sites.

Table 2. Seasonal vegetation development dynamics within a growing period.

Measurement Date	Plot A [m^2]	Plot A (% of Area)	Plot B [m^2]	Plot B (% of Area)	Plot C [m^2]	Plot C (% of Area)
Baseline (1 August 2024)	17.03	6%	3.17	1%	1.55	1%
Spring Peak (30 May 2025)	73.68	26%	52.33	19%	101.18	36%
Mid-season Stress (26 June 2025)	47.69	17%	27.11	10%	39.97	14%
July Peak (31 July 2025)	204.83	73%	225.36	80%	265.35	94%
Late Summer (21 August 2025)	37.13	30%	49.14	26%	108.44	47%

The decline in coverage observed in mid-June (26 June 2025) may indicate a period of hydrological stress typical of the transition between moisture availability phases on sites with limited water retention capacity. In this study, the lack of rain contributed to the observed situation.

The distinct spatial variability among the plots suggests heterogeneity in site and soil conditions typical of post-mining areas. The progressive decline in coverage in late August remains consistent with the phenological transition toward autumn and serves as a reference point for monitoring long-term trends in ecosystem regeneration.

In comparison with satellite-based methodologies [25], the present UAV-based approach facilitates significantly more precise NDVI estimation at the plot scale, particularly in experimental areas of small size. A related study on UAV monitoring of post-mining effects [4] primarily concentrated on terrain deformation and broader environmental indicators, rather than achieving such fine-grained vegetation quantification. The present study contributes to the advancement of the application by combining high spatial resolution with automated NDVI-based classification, thus enhancing both sensitivity and reproducibility. Regarding the NDVI-based vegetation assessment, the results obtained are consistent with those reported in other UAV-based vegetation monitoring studies [35,41].

The proposed UAV-based NDVI monitoring framework shows strong potential for practical implementation in adaptive reclamation management. The frequent flight campaigns and the high spatial resolution of UAV surveys enable early detection of vegetation stress, allowing timely interventions such as targeted irrigation, soil amendment, or reseeding before degradation becomes irreversible. This proactive capability is particularly valuable in heterogeneous post-mining environments, where localized failures may otherwise remain undetected using conventional monitoring approaches.

Furthermore, the automated and reproducible UAV–QGIS workflow supports transparent environmental reporting, providing quantitative indicators that can be integrated into regulatory compliance frameworks and certification schemes. Such data-driven monitoring systems can enhance stakeholder confidence, facilitate performance benchmarking across sites, and contribute to the standardization of reclamation assessment practices within the broader context of post-mining land management and the European Green Deal objectives.

5. Conclusions

The study demonstrates that high-resolution UAV-based multispectral monitoring, combined with an automated QGIS processing workflow, provides a robust and operationally scalable method for quantifying vegetation recovery on heterogeneous post-mining waste heaps. The developed UAV–QGIS workflow successfully enabled systematic, biweekly monitoring of seasonal vegetation dynamics at approximately 4 cm/pixel spatial resolution, ensuring high sensitivity to small-scale spatial variability typical of coal mine

https://doi.org/10.3390/su18094583

heaps. The automation of reprojection, clipping, NDVI thresholding (NDVI $\geq$ 0.2), and vegetation area calculation significantly reduced manual processing requirements and improved reproducibility and analytical transparency.

The results of the application of the methodology developed in the Jankowice mine heap indicated the following:

- Baseline measurements conducted in August 2024 confirmed extremely low initial vegetation cover across all monitored plots (below 6%). This indicated that spontaneous succession alone was insufficient for rapid ecological stabilization of the substrate.
- The comparative analysis of three reclamation treatments revealed big treatment-dependent differences in vegetation establishment. Seeding alone showed the weakest performance, with limited vegetation cover and higher vulnerability to seasonal stress. Seeding and irrigation demonstrated moderate improvement over seeding alone, indicating that additional water supply partially mitigates substrate limitations. Finally, compost-amended treatment maintained the highest level of vegetation cover and significantly surpassed both seeding-only treatments and treatment combining seeding with irrigation.
- Temporal analysis showed synchronized seasonal dynamics across all plots, with rapid expansion during late spring and early summer (May–July 2025), followed by a sharp decline in August due to combined phenological transition and extreme heat/drought stress. However, Plot C demonstrated greater resilience in absolute coverage levels even during stress periods.

The results confirm that high-frequency UAV monitoring enables the detection of both peak performance and stress-induced decline, supporting adaptive reclamation management. Automated open-source geoprocessing workflows can provide transparent, reproducible, and regulator-ready performance indicators.

It should be noted that the present study does not include an assessment of plant species composition or relative abundance within the study plots. The developed UAV-based NDVI approach provides quantitative information on vegetation cover and its temporal changes but does not enable species analysis. Although such information is important for evaluating ecological succession, substrate stabilization, and resistance to erosion, its acquisition typically requires ground-based surveys or advanced classification methods. Future work will aim to integrate species-level analysis to complement the NDVI-based monitoring framework and support a more comprehensive evaluation of reclamation outcomes.

In addition, future research will incorporate ground-based measurements such as biomass sampling, vegetation cover estimation, and plant density assessments to validate UAV-derived NDVI results. Moreover, the integration of UAV data with satellite platforms could enable hybrid multi-scale monitoring applicable at full-heap and regional levels, supporting standardized performance indicators aligned with ecological certification and post-mining transition frameworks.

Supplementary Materials: The following supporting information can be downloaded at: https://www.mdpi.com/article/10.3390/su18094583/s1, Figure S1: DJI Mavic 3 Multispectral; Figure S2: (Above) Performing a flight over the KWK ROW Ruch Jankowice mine heap (Belowm) Flight path over the chosen mine heap, displayed on DJI Controller; Figure S3: (Above) Flight path over chosen mine heap. DJI Controller, (Below) DJI Terra software view—multispectral orthophoto containing graphical interpretation. Source: Authors' own work base on DJI Terra Software; Figure S4: Diagram showing the steps for NDVI calculation as developed in QGIS Modeler. Source: Authors' own work based on QGIS Modeler Software; Figure S5: (Above) Algorithm execution progress window. Source: Authors' own work based on QGIS Modeler Software; (Below) Attribute tables. Source: Authors' own work based on QGIS Software. Details on equipment and software used are provided in the Supplementary Materials.

Author Contributions: Conceptualization, B.O., M.G., D.M. and J.T.; methodology, B.O., D.M., E.A.V. and M.G.; software, B.O. and D.M.; validation, K.S., M.G. and E.A.V.; investigation, B.O., K.S. and J.T.; data curation, B.O., D.M. and J.T.; writing—original draft preparation, B.O. and M.R.; writing—review and editing, B.O., M.R., J.T., G.X., E.A.V. and K.S.; visualization, K.S.; project administration, D.M.; funding acquisition, M.G., E.A.V., D.M., J.T., K.S. and M.R. All authors have read and agreed to the published version of the manuscript.

Funding: This work is based on research within the RFCS project REECOL, which is a project co-funded by the EU under GA No. 101112657.

Institutional Review Board Statement: Not applicable.

Informed Consent Statement: Not applicable.

Data Availability Statement: The original contributions presented in this study are included in the article. Further inquiries can be directed to the corresponding author.

Conflicts of Interest: The authors declare no conflicts of interest.

References

1. European Commission. Communication from the Commission to the European Parliament, the European Council, the Council, the European Economic and Social Committee and the Committee of the Regions—The European Green Deal (COM(2019) 640 Final). Available online: https://eur-lex.europa.eu/legal-content/EN/TXT/?uri=CELEX:52019DC0640 (accessed on 10 November 2025).
2. Malec, M.; Stańczak, L.; Ricketts, B. Just transition of post mining areas—Technical, economic, environmental and social aspects. *Min. Mach.* **2023**, *41*, 25–33. [CrossRef]
3. Vervoort, A.; Declercq, P.-Y. Upward surface movement above deep coal mines after closure and flooding of underground workings. *Int. J. Min. Sci. Technol.* **2018**, *28*, 53–59. [CrossRef]
4. Pawlik, M.; Haske, B.; Flores, H.; Bernsdorf, B.; Rudolph, T. Towards a Long-Term Unmanned Aerial Vehicle (UAV) Monitoring Framework for Post-Mining Effects: Prosper-Haniel Case. *Mining* **2024**, *4*, 211–229. [CrossRef]
5. Sheoran, V.; Sheoran, A.S.; Poonia, P. Soil Reclamation of Abandoned Mine Land by Revegetation: A Review. *Int. J. Soil Sediment Water* **2010**, *3*, 13.
6. Shao, Y.; Xu, Q.; Wei, X. Progress of mine land reclamation and ecological restoration research based on bibliometric analysis. *Sustainability* **2023**, *15*, 10458. [CrossRef]
7. Woźniak, G.; Bakar, J.; Dyczko, A.; Jarosz, J.; Ryś, K.; Radosz, Ł.; Kaul, S.; Adamik, K.; Besenyei, L.; Prostański, D. The diversity and plant species composition of the spontaneous vegetation on coal mine spoil heaps in relation to the area size. *Min. Mach.* **2023**, *1*, 68–84. [CrossRef]
8. Hendrychová, M.; Svobodova, K.; Kabrna, M. Mine reclamation planning and management: Integrating natural habitats into post-mining land use. *Resour. Policy* **2020**, *69*, 101882. [CrossRef]
9. Biegańska, J.; Tora, B.; Sinka, T.; Čablík, V.; Hlavatá, M. Reclamation and Revitalization of Post-Mining Sites—Ups and Downs. *Acta Montan. Slovaca* **2023**, *28*, 637–654. [CrossRef]
10. Wu, X.; Xing, C.; Ju, Q.; Su, S.; Zhang, X.; Zhu, T. Research progress in mining ecological restoration technology. *J. Ind. Saf.* **2024**, *1*, 100004. [CrossRef]
11. Navarro-Ramos, S.E.; Sparacino, J.; Rodríguez, J.M.; Filippini, E.; Marsal-Castillo, B.E.; García-Cannata, L.; Renison, D.; Torres, R.C. Active revegetation after mining: What is the contribution of peer-reviewed studies? *Heliyon* **2022**, *8*, e09179. [CrossRef]
12. United Nations. *Transforming Our World: The 2030 Agenda for Sustainable Development*; Resolution A/RES/70/1; United Nations: New York, NY, USA, 2015. Available online: https://www.un.org/sustainabledevelopment/sustainable-development-goals/ (accessed on 10 April 2026).
13. Audet, P.; Gravina, A.; Glenn, V.; McKenna, P.; Vickers, H.; Gillespie, M.; Mulligan, D. Structural Development of Vegetation on Rehabilitated North Stradbroke Island: Above/Belowground Feedback May Facilitate Alternative Ecological Outcomes. *Ecol. Process.* **2013**, *2*, 20. [CrossRef]
14. Macagga, R.; Sossa, G.; Ayaribil, Y.; Bayot, R.; Sanchez, P.; Augustin, J.; Bellingrath-Kimura, S.D.; Hoffmann, M. A new, low-cost ground-based NDVI sensor for manual and automated crop monitoring. *Smart Agric. Technol.* **2025**, *11*, 100892. [CrossRef]

15. Tucker, C.J. Red and photographic infrared linear combinations for monitoring vegetation. *Remote Sens. Environ.* **1979**, *8*, 127–150. [CrossRef]
16. Knipling, E.B. Physical and physiological basis for the reflectance of visible and near-infrared radiation from vegetation. *Remote Sens. Environ.* **1970**, *1*, 155–159. [CrossRef]
17. Auravant. Vegetation Indices and Their Interpretation: NDVI, GNDVI, MSAVI2, NDRE, and NDWI. Available online: https://www.auravant.com/en/articles/precision-agriculture/vegetation-indices-and-their-interpretation-ndvi-gndvi-msavi2-ndre-and-ndwi/ (accessed on 1 December 2025).
18. Nafarin, N.A.; Novitasari, N. Relationship between normalized difference vegetation index (NDVI) and rice growth phases. *IOP Conf. Ser. Earth Environ. Sci.* **2023**, *1184*, 012034. [CrossRef]
19. Vescovo, L.; Wohlfahrt, G.; Balzarolo, M.; Pilloni, S.; Sottocornola, M.; Rodeghiero, M.; Gianelle, D. New spectral vegetation indices based on the near-infrared shoulder wavelengths for remote detection of grassland phytomass. *Int. J. Remote Sens.* **2012**, *33*, 2178–2195. [CrossRef]
20. Rouse, J.W.; Haas, R.H.; Schell, J.A.; Deering, D.W.; Harlan, J.C. *Monitoring the Vernal Advancements and Retrogradation (Greenwave Effect) of Nature Vegetation*; NASA/GSFC Final Report; NASA: Greenbelt, MD, USA, 1974.
21. Luo, W.; Qiu, H.; Wei, Y.; Huangfu, W.; Yang, D. A proposed method for landslide detection based on transfer learning and graph neural network. *Geosci. Front.* **2025**, *16*, 102171. [CrossRef]
22. Peng, S.; Bao, N.; Gu, N.; Qian, H.; Han, Z.; Zhou, B.; Chang, L. Enhanced assessment of chlorophyll-a and total nitrogen dynamics using unmanned aerial vehicle-based model and hyperspectral imagery in coastal wetland water. *Environ. Technol. Innov.* **2025**, *40*, 104521. [CrossRef]
23. McKenna, P.B.; Lechner, A.M.; Phinn, S.; Erskine, P.D. Remote Sensing of Mine Site Rehabilitation for Ecological Outcomes: A Global Systematic Review. *Remote Sens.* **2020**, *12*, 3535. [CrossRef]
24. Karan, S.; Samadder, S.; Maiti, S. Assessment of the capability of remote sensing and GIS techniques for monitoring reclamation success in coal mine degraded lands. *J. Environ. Manag.* **2016**, *182*, 272–283. [CrossRef]
25. Varouchakis, E.A.; Komnitsas, K.; Galetakis, M. Spatiotemporal Analysis of Vegetation Health and Moisture Dynamics in Rehabilitated Mining Quarries Using Satellite Imagery. *Environ. Process.* **2025**, *12*, 45. [CrossRef]
26. Buczyńska, A. Remote sensing and GIS technologies in land reclamation and landscape planning processes on post-mining areas in the Polish and world literature. *AIP Conf. Proc.* **2020**, *2209*, 040002. [CrossRef]
27. Buczyńska, A.; Blachowski, J.; Bugajska-Jędraszek, N. Analysis of Post-Mining Vegetation Development Using Remote Sensing and Spatial Regression Approach: A Case Study of Former Babina Mine (Western Poland). *Remote Sens.* **2023**, *15*, 719. [CrossRef]
28. Smentek, A.; Blachowski, J. Remote Sensing Analysis of Environmental Changes in a Post-Mining Area: A Case Study of the Olkusz Region—Preliminary Results. *Civ. Environ. Eng. Rep.* **2025**, *35*, 1–18. [CrossRef]
29. Hu, J.; Ye, B.; Bai, Z.; Feng, Y. Remote Sensing Monitoring of Vegetation Reclamation in the Antaibao Open-Pit Mine. *Remote Sens.* **2022**, *14*, 5634. [CrossRef]
30. Juanda, E.T.; Martono, D.N.; Saria, L. Analysis vegetation change on coal mine reclamation using Normalized Difference Vegetation Index (NDVI). *IOP Conf. Ser. Earth Environ. Sci.* **2021**, *716*, 012035. [CrossRef]
31. O'Donnell, M.S.; Whipple, A.L.; Inman, R.D.; Tarbox, B.C.; Monroe, A.P.; Robb, B.S.; Aldridge, C.L. *Remote Sensing for Monitoring Mine Lands and Recovery Efforts: U.S. Geological Survey Circular 1525*; U.S. Geological Survey: Fort Collins, CO, USA, 2024. [CrossRef]
32. Jiang, X.; Gao, Y.; Wu, L.; Li, H. Dynamic monitoring of vegetation restoration in coal mining subsidence area: A case in Jiawang District, Xuzhou City. In *Proceedings of the Fifth International Conference on Geoscience and Remote Sensing Mapping (ICGRSM 2023), Lianyungang, China, 13–15 October 2023*; SPIE: Bellingham, WA, USA, 2023. [CrossRef]
33. Smith, H.W.; Ashworth, A.J.; King, S.; Kreman, C.; Miller, D.M.; Nalley, L.L.; Owens, P.R. Remote sensing reveals trends in vegetative recovery and land cover transformation post-reclamation at Tar Creek Superfund Site. *Discov. Geosci.* **2024**, *2*, 53. [CrossRef]
34. Li, J.; Chen, B. Global Revisit Interval Analysis of Landsat-8 -9 and Sentinel-2A -2B Data for Terrestrial Monitoring. *Sensors* **2020**, *20*, 6631. [CrossRef]
35. Nugraha, A.P.; Hariyanto, T. Evaluation of Vegetation Health in the PT X Reclamation Area Using the NDVI Method Based on Unmanned Aerial Vehicle (UAV) Multispectral Orthophoto Data. *IOP Conf. Ser. Earth Environ. Sci.* **2024**, *1418*, 012010. [CrossRef]
36. Phang, S.K.; Ren, H.; Choy, S.; Wang, X.; Li, Y.; Zhang, L. From Satellite to UAV-Based Remote Sensing: A Review. *IEEE Geosci. Remote Sens. Mag.* **2023**, *11*, 127057–127076. [CrossRef]
37. Berni, J.; Zarco-Tejada, P.; Suarez, L.; Fereres, E. Remote sensing of vegetation from UAV platforms using lightweight multispectral and thermal imaging sensors. *Int. Arch. Photogramm. Remote Sens. Spat. Inf. Sci.* **2014**, *38*, 6.
38. Anderson, J.; Iverson, M.; Pearse, B. Applications for remote sensing by unmanned aerial vehicles in reclamation monitoring. In *Proceedings of the British Columbia Mine Reclamation Symposium*; University of British Columbia Library: Vancouver, BC, Canada, 2021. [CrossRef]

39. Buters, T.M.; Bateman, P.W.; Robinson, T.; Belton, D.; Dixon, K.W.; Cross, A.T. Methodological Ambiguity and Inconsistency Constrain Unmanned Aerial Vehicles as A Silver Bullet for Monitoring Ecological Restoration. *Remote Sens.* **2019**, *11*, 1180. [CrossRef]
40. Haskins, J.; Endris, C.; Thomsen, A.S.; Gerbl, F.; Fountain, M.C.; Wasson, K. UAV to Inform Restoration: A Case Study from a California Tidal Marsh. *Front. Environ. Sci.* **2021**, *9*, 642906. [CrossRef]
41. Chen, R.; Han, L.; Zhao, Y.; Zhao, Z.; Liu, Z.; Li, R.; Xia, L.; Zhai, Y. Extraction and monitoring of vegetation coverage based on uncrewed aerial vehicle visible image in a post gold mining area. *Front. Ecol. Evol.* **2023**, *11*, 1171358. [CrossRef]
42. Zhao, Y.; Zheng, W.; Xiao, W.; Zhang, S.; Lv, X.; Zhang, J. Rapid monitoring of reclaimed farmland effects in coal mining subsidence area using a multi-spectral UAV platform. *Environ. Monit. Assess.* **2020**, *192*, 474. [CrossRef]
43. Park, S.; Choi, Y. Applications of Unmanned Aerial Vehicles in Mining from Exploration to Reclamation: A Review. *Minerals* **2020**, *10*, 663. [CrossRef]
44. Yamaguchi, T.; Sasano, K.; Katsura, K. Improving efficiency of ground-truth data collection for UAV-based rice growth estimation models: Investigating the effect of sampling size on model accuracy. *Plant Prod. Sci.* **2024**, *27*, 1–13. [CrossRef]
45. Markov, N.; Yorgov, D.; Veleva, P.; Petrova, A.; Atanasova, A. Assessing the applicability of drone-mounted multispectral camera measurements to characterize wheat status during the vegetation. *Agric. Sci. Technol.* **2025**, *17*, 81–86. [CrossRef]
46. Verterra. Harnessing UAV Technology to Improve Mine Rehabilitation Outcomes. Verterra Insights. 2025. Available online: https://www.verterra.com.au/insights/harnessing-uav-technology-to-improve-mine-rehabilitation-outcomesnbsp (accessed on 20 December 2025).
47. Strohbach, B.J.; Hauptfleisch, M.L.; Green-Chituti, A.; Diener, S.M. Determining rehabilitation effectiveness at the Otjikoto Gold Mine, Otjozondjupa Region, Namibia, using high-resolution NIR aerial imagery. *Namib. J. Environ.* **2018**, *2*, 134–146. [CrossRef]
48. Czyża, S.; Szuniewicz, K.; Kowalczyk, K.; Dumalski, A.; Ogrodniczak, M.; Zieleniewicz, Ł. Assessment of Accuracy in Unmanned Aerial Vehicle (UAV) Pose Estimation with the REAL-Time Kinematic (RTK) Method on the Example of DJI Matrice 300 RTK. *Sensors* **2023**, *23*, 2092. [CrossRef]
49. González-García, J.; Swenson, R.L.; Gómez-Espinosa, A. Real-time kinematics applied at unmanned aerial vehicles positioning for orthophotography in precision agriculture. *Comput. Electron. Agric.* **2020**, *177*, 105695. [CrossRef]
50. Niu, Z.; Xia, H.; Tao, P.; Ke, T. Accuracy assessment of UAV photogrammetry system with RTK measurements for direct georeferencing. *ISPRS Ann. Photogramm. Remote Sens. Spat. Inf. Sci.* **2024**, *X-1-2024*, 169–176. [CrossRef]
51. RTKData. Drones. Available online: https://rtkdata.com/drones/ (accessed on 21 November 2025).
52. Syetiawan, A.; Pranoto, F.S.; Pratama, R.A.; Prihatin, S.M. High Accuracy Rapid Mapping Using NTRIP-RTK on Unmanned Aerial Vehicle. In *Proceedings of the 2024 IEEE International Conference on Aerospace Electronics and Remote Sensing Technology (ICARES), Yogyakarta, Indonesia, 8–9 November 2024*; IEEE: Piscataway, NJ, USA, 2024.
53. Whomsley, M.; Booth, K. Comparative accuracy of GNSS, NTRIP, and base station UAV surveys. In *Proceedings of the FIG Working Week 2025: Collaboration, Innovation and Resilience: Championing a Digital Generation, Brisbane, Australia, 6–10 April 2025*; International Federation of Surveyors (FIG): Copenhagen, Denmark, 2025.
54. Worsa-Kozak, M.; Górniak-Zimroz, J.; Szrek, A.; Chudy, K. Remote Detection and Monitoring of Post-Mining Heat Island. *Front. Environ. Sci.* **2024**, *12*, 1305149. [CrossRef]
55. He, X.; Yang, X.; Luo, Z.; Guan, T. Application of Unmanned Aerial Vehicle (UAV) Thermal Infrared Remote Sensing to Identify Coal Fires in the Huojitu Coal Mine in Shenmu City, China. *Sci. Rep.* **2020**, *10*, 13895. [CrossRef]
56. Teodoro, A.C.; Fernandes, J.; Santos, P.; Duarte, L.; Flores, D. Evaluation of temperature in a self-burning coal waste pile considering UAV data and in situ measurements. In *Proceedings of the 2020 IEEE International Geoscience and Remote Sensing Symposium (IGARSS), Waikoloa, HI, USA, 26–31 July 2020*; IEEE: Piscataway, NJ, USA, 2020; pp. 5218–5221. [CrossRef]
57. Jabłońska, K.; Maksymowicz, M.; Tanajewski, D.; Kaczan, W.; Zięba, M.; Wilgucki, M. MineCam: Application of Combined Remote Sensing and Machine Learning for Segmentation and Change Detection of Mining Areas Enabling Multi-Purpose Monitoring. *Remote Sens.* **2024**, *16*, 955. [CrossRef]
58. Gu, Z.; Zeng, M. The Use of Artificial Intelligence and Satellite Remote Sensing in Land Cover Change Detection: Review and Perspectives. *Sustainability* **2024**, *16*, 274. [CrossRef]
59. Do, T.P.T.; Nguyen, L.Q.; Trinh, L.H.; Vambol, V. Comprehensive Review of Unmanned Aerial Vehicle Application to Safety Mining Management. *Ecol. Quest.* **2024**, *35*, 69–90. [CrossRef]
60. Mpanza, M.; Wistockk, J.; Rupprecht, S. Mapping tailings storage facilities associated with abandoned mine sites. In *Proceedings of the Mine Closure 2024: 17th International Conference on Mine Closure, Perth, Australia, 26–28 November 2024*; Australian Centre for Geomechanics: Perth, Australia, 2024. [CrossRef]
61. Han, Y.; Zhang, S.; Dai, C.; Peng, J.; Chen, Y.; Ke, H. Estimating Soil Cadmium Concentration Using Multi-Source UAV Imagery and Machine Learning Techniques. *Environ. Monit. Assess.* **2025**, *197*, 583. [CrossRef] [PubMed]
62. Pawlik, M.; Nguy, Q.A.; Bernsdorf, B.; Rudolph, T.; Haske, B. The Use of Multisensor Drone Monitoring to Fault Zones in Areas Affected by Mining Activities. *Civ. Environ. Eng. Rep.* **2025**, *35*, 108. [CrossRef]

63. Siegmund, M.; Bałaga, D.; Roumpos, C.; Servou, A.; Gkoutzou, A.; Hullot, O. Automated Spraying System for Post-Mining Land Reclamation—Structural Design and Functional Testing. *Min. Mach.* **2025**, *43*, 254–268. [CrossRef]
64. Joubert-van der Merwe, L.; Samways, M.J.; Pryke, J.S. A new protocol for monitoring operational outcomes of environmental management in commercial forestry plantations. *J. Environ. Manag.* **2025**, *271*, 110922. [CrossRef]
65. Zheng, J.; Tan, J.; Chen, G. Research on UAV coverage path planning in building visual inspection. *J. Build. Eng.* **2025**, *111*, 113556. [CrossRef]
66. Mian, O.; Lutes, J.; Lipa, G.; Hutton, J.J.; Gavelle, E.; Borghini, S. Direct Georeferencing on Small Unmanned Aerial Platforms for Improved Reliability and Accuracy of Mapping Without the Need for Ground Control Points. *Int. Arch. Photogramm. Remote Sens. Spat. Inf. Sci.* **2015**, *XL-1/W4*, 397–402. [CrossRef]
67. Zambrano, P.; Calderon, F.; Villegas, H.; Corredores, J.P.; Pazmiño, D.; Realpe, M. UAV Remote Sensing applications and current trends in crop monitoring and diagnostics: A Systematic Literature Review. In *Proceedings of the 2023 IEEE 13th International Conference on Pattern Recognition Systems (ICPRS)*; IEEE: Piscataway, NJ, USA, 2023; Volume 1, p. 9. [CrossRef]
68. Corder, G.W.; Foreman, D.I. *Nonparametric Statistics: A Step-by-Step Approach*; Wiley: Hoboken, NJ, USA, 2014.

https://doi.org/10.3390/su18094583